Biochemical and Biophysical Research Communications 447 (2014) 101–107

Contents lists available at ScienceDirect

Biochemical and Biophysical Research Communications

journal homepage: www.elsevier.com/locate/ybbrc

Structural and kinetic bases for the metal preference of the M18 aminopeptidase from *Pseudomonas aeruginosa*

Duy Duc Nguyen [a], Ramesh Pandian [a], Doyoun Kim [a], Sung Chul Ha [b], Hye-Jin Yoon [c], Kap Sun Kim [a], Kyung Hee Yun [a], Jin-Hahn Kim [a,*], Kyeong Kyu Kim [a,*]

[a] Department of Molecular Cell Biology, Samsung Biomedical Research Institute, Sungkyunkwan University School of Medicine, Suwon 440-746, Republic of Korea
[b] Pohang Acceleratory Laboratory, Pohang University of Science and Technology, Pohang, Kyungbuk 790-784, Republic of Korea
[c] Department of Chemistry, College of Natural Sciences, Seoul National University, Seoul 157-747, Republic of Korea

ARTICLE INFO

Article history:
Received 20 March 2014
Available online 1 April 2014

Keywords:
M18 family
Aspartyl aminopeptidase
Enzyme kinetics
Tetrahedral aminopeptidase
Pseudomonas aeruginosa

ABSTRACT

The peptidases in clan MH are known as cocatalytic zinc peptidases that have two zinc ions in the active site, but their metal preference has not been rigorously investigated. In this study, the molecular basis for metal preference is provided from the structural and biochemical analyses. Kinetic studies of *Pseudomonas aeruginosa* aspartyl aminopeptidase (PaAP) which belongs to peptidase family M18 in clan MH revealed that its peptidase activity is dependent on Co^{2+} rather than Zn^{2+}: the k_{cat} (s^{-1}) values of PaAP were 0.006, 5.10 and 0.43 in no-metal, Co^{2+}, and Zn^{2+} conditions, respectively. Consistently, addition of low concentrations of Co^{2+} to PaAP previously saturated with Zn^{2+} greatly enhanced the enzymatic activity, suggesting that Co^{2+} may be the physiologically relevant cocatalytic metal ion of PaAP. The crystal structures of PaAP complexes with Co^{2+} or Zn^{2+} commonly showed two metal ions in the active site coordinated with three conserved residues and a bicarbonate ion in a tetragonal geometry. However, Co^{2+}- and Zn^{2+}-bound structures showed no noticeable alterations relevant to differential effects of metal species, except the relative orientation of Glu-265, a general base in the active site. The characterization of mutant PaAP revealed that the first metal binding site is primarily responsible for metal preference. Similar to PaAP, *Streptococcus pneumonia* glutamyl aminopeptidase (SpGP), belonging to aminopeptidase family M42 in clan MH, also showed requirement for Co^{2+} for maximum activity. These results proposed that clan MH peptidases might be a cocatalytic cobalt peptidase rather than a zinc-dependent peptidase.

1. Introduction

Protein degradation, one of the most important processes determining the outcome of many biological signaling pathways, is conducted by peptidases [1], which can be classified into several clans according to the MEROPS database [2]. A clan comprises peptidases that have arisen from a single evolutionary origin, and is further subdivided into families based on structural similarity, the order of catalytic-site residues, or, often, sequence motifs around the catalytic residues. In MEROPS classification, the M18, M20, M28, and M42 families comprise clan MH, and peptidases belonging to this clan are known as zinc-dependent exopeptidases. However, clear characterizations of enzymatic properties of MH exopeptidases are surprisingly sparse. Family M18, in which the founding member was yeast aminopeptidase I (MEROPS ID: M18.001) [3] and firstly identified from mammalian by Wilk et al. [4], is widely distributed in bacteria and eukaryotes and consists of metalloaminopeptidases which utilize metal ions to facilitate the removal of N-terminal acidic amino acids in peptide substrates. So far, small numbers of peptidases in this family have been characterized in detail: yeast aminopeptidase I (MEROPS ID: M18.001) [3], mammalian aspartyl aminopeptidase (MEROPS ID: M18.002) [4–6], and aminopeptidase from *Plasmodium falciparum* [7]. Aminopeptidase from *Pseudomonas aeruginosa* (PaAP), which also belongs to the M18 peptidase family, is predicted to be an aspartyl aminopeptidase (E.C. 3.4.11.21), but its biochemical properties have not been investigated yet.

The two metal ions in the active site of metalloaminopeptidases are notated as [M1M2-enzyme], where M1 represents the cocatalytic metal which is near the active site, and M2 is a structural metal adjacent to the substrate binding pocket [8]. Although the general reaction mechanism of the bimetallic aminopeptidases has been proposed [8], each enzyme seems to be quite different from the others. For example, although the reaction is commonly

* Corresponding authors.
E-mail addresses: jhahnkim@skku.edu (J.-H. Kim), kyeongkyu@skku.edu (K.K. Kim).

http://dx.doi.org/10.1016/j.bbrc.2014.03.109
0006-291X/

Table 1
Data collection and refinement statistics.

	[Co1Co2-(PaAP)]	[Zn1Zn2-(PaAP)]	[W1-D236A]	[Zn1W2-H82A]
Data collection				
Beam lines	7A (PAL)	4A (PAL)	4A (PAL)	PF17A (Spring8)
Space group	*H3*	*H3*	*H3*	*C2221*
Unit-cell parameters (Å,°)	$a = b = 133.21$	$a = b = 134.19$	$a = b = 133.61$	$a = 150.02$
	$c = 322.32$	$c = 328.76$	$c = 320.96$	$b = 218.27$
	$\alpha = \beta = 90$	$\alpha = \beta = 90$	$\alpha = \beta = 90$	$c = 172.69$
	$\gamma = 120$	$\gamma = 120$	$\gamma = 120$	$\alpha = \beta = \gamma = 90$
Resolution (Å)	50.00–2.70 (2.80–2.70)[a]	30.00–2.30 (2.34–2.30)	50.00–2.30 (2.34–2.30)	50.00–2.45 (2.49–2.45)
R_{merge}[b] (%)	9.40 (44.20)	10.30 (37.40)	7.60 (25.80)	6.20 (17.50)
I/σ (I)	12.64 (2.13)	11.08 (2.28)	12.59 (2.91)	42.58 (6.90)
Completeness (%)	98.50 (96.10)	100 (100)	98.50 (99.30)	95.90 (62.90)
Multiplicity	3.5 (3.3)	3.2 (3.2)	2.0 (2.0)	7.2 (5.8)
Refinement				
No. of reflections	57527	98152	93257	100620
R_{work}/R_{free}[c] (%)	0.17/0.22	0.15/0.20	0.15/0.20	0.15/0.21
No. of atoms in Proteins	12652	13029	12286	18936
No. of atoms in Ligands/ions	63	24	0	6
No. Waters	103	913	629	890
B factor (Å^2)	42.0	28.5	32.2	39.5
RMSD bonds (Å)/angles(°)	0.008/1.21	0.018/1.92	0.019/1.94	0.015/1.74
Ramachandran plot[d] (%)	95.1/3.9/1.1	95.6/3.5/0.9	96.2/3.2/0.6	95.1/4.4/0.5

[a] The value in parentheses of resolution range, completeness, R_{merge} and I/σ (I) correspond to the last shell.
[b] R_{merge} $(I) = \Sigma_{hkl}\Sigma_j[|I(hkl)_j - I(hkl)|]/[\Sigma_{hkl} I_{hkl}]$, is the jth measurement of the intensity of reflection hkl and $< I(hkl)>$ is the average intensity.
[c] $R = \Sigma_{hkl}||F_{obs}| - |F_{calc}||/\Sigma_{hkl}|F_{obs}|$. Where R_{free} is calculated without a sigma cutoff for a randomly chosen 5% of reflections, which were not used for structure refinement, and R_{work} is calculated for the remaining reflections.
[d] Percentage of residues in favored region/allowed region/outlier region.

Table 2
Michaelis-Menten parameters and reaction constants for M18 PaAP and M42 SpGP in the presence and absence of transition metal ions.

Metal	k_{cat} (s^{-1})		k_{cat}/K_M ($s^{-1}M^{-1}$)		K_M (mM)	
	M18 PaAp	M42 PepA	M18 PaAp	M42 PepA	M18 PaAp	M42 PepA
No metal	0.006 ± 0.0001	0.01 ± 0.002	40	19	0.16 ± 0.02	0.53 ± 0.08
Mn^{2+}	5.46 ± 0.60	2.78 ± 0.07	7800	1100	0.70 ± 0.18	2.6 ± 0.37
Co^{2+}	5.10 ± 0.33	5.3 ± 1.9	6200	3300	0.82 ± 0.18	1.6 ± 0.83
Ni^{2+}	0.81 ± 0.04	1.2 ± 0.18	2989	441	0.28 ± 0.06	2.6 ± 0.46
Zn^{2+}	0.43 ± 0.05	0.54 ± 0.06	855	607	0.53 ± 0.16	0.89 ± 0.10
Cu^{2+}	0.14 ± 0.01	0.30 ± 0.07	392	285	0.36 ± 0.03	1.0 ± 0.17

initiated by nucleophilic water [9], the locations of the residues serving as general bases are diverse [9,10]. Furthermore, the metal preferences and the role of each metal site for the bimetallic aminopeptidase and those of M18 are not well elucidated yet. It is known that the cocatalytic metal can be replaced, and that enzymatic activity is significantly affected by the metallic species [11]. For example, some leucine aminopeptidases (E.C. 3.4.11.1) lose their activity following dialysis against Cd^{2+}-containing buffer or stoichiometric treatment of 1,10-phenanthroline [12,13] Given this, it is worthwhile to investigate the metal preference of peptidases belonging to clan MH even though they are defined as zinc proteases in MEROPS [2], on the hypothesis that metals other than Zn^{2+} can be recruited to the active site of metalloaminopeptidases in physiological conditions, because the affinities of M1-M2 sites for various metal ions in a variety of aminopeptidases are broad with K_d's in the subnanomolar to millimolar range [8]. As expected, it has been found that mammalian tetrahedral aspartyl aminopeptidases belonging to the M18 family show different metal selectivity [5,6]. However, metal preferences of aminopeptidases must be considered in physiological conditions to understand their cellular functions. For example, methionine aminopeptidase (E.C. 3.4.11.18) is proposed to work as a zinc-peptidase *in vivo* since enzymatic activity is conferred only by zinc ions in a physiological concentration of reduced glutathione [14]. However, ferrous ion was determined as a cofactor later by inductively coupled plasma emission analysis [15]. Structural studies have also provided clues to understand metal preferences as well as catalytic mechanisms [6,16]. In this study, we attempted to answer the question of the metal preference of MH clan peptidases using M18 aspartyl aminopeptidase from *Pseudomonas aeruginosa* (PaAP) as a model peptidase. To comprehensively understand the metal preference of PaAP, we performed kinetic measurements and structure determination of PaAP.

2. Materials and methods

2.1. Protein preparation

The gene PA3247, encoding the M18 aminopeptidase, was amplified by PCR using *P. aeruginosa* genomic DNA and cloned into the pVFT1S vector. H82A, H401A and D236A mutants were made by site-directed mutagenesis. The wild-type and mutant proteins were expressed and purified using the same procedures. Proteins were expressed in *Escherichia coli* BL21 (DE3) cells at 37 °C, and purified using HiTrap™ chelating and Q columns (GE Healthcare). The detailed purification protocols are described in Supplementary materials. The purified proteins were concentrated using Centricon (Millipore) to 12 mg/ml concentration. Protein purity was analyzed by SDS-PAGE. In order to reintroduce metal ions to PaAP's catalytic site, specific metal ions were added to the final buffer at a final concentration of 0.1 mM.

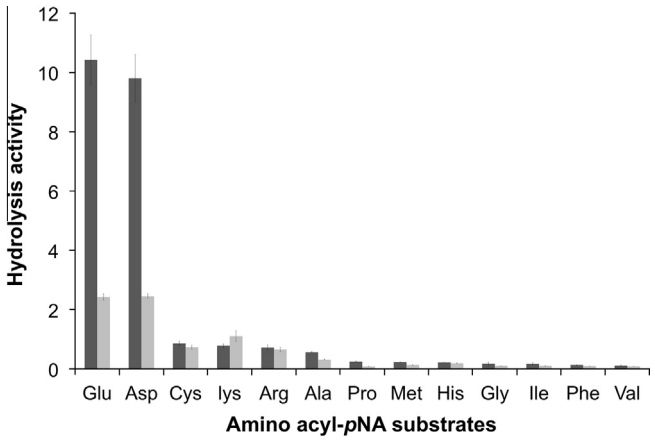

Fig. 1. Substrate specificity of PaAP. 5 μM enzyme was mixed with 500 μM substrate in 100 mM Hepes pH 7.5 and 0.1 mM Co^{2+} (black) and Zn^{2+} (gray) at 37 °C. The released of *p*-nitroaniline was monitored by measuring absorbance at 405 nm for 5 min. The hydrolysis activity was calculated by converting absorbance to μmol of product per g of enzyme per second. Data represent average values with error bars from three independent experiments.

2.2. Structure determination

The wild-type and D236A crystals were formed in 30% PEG 400, 0.1 M Tris pH 8.0, 0.2 M $MgCl_2$, and 0.1 mM $ZnCl_2$. The cobalt-bound proteins were crystallized in the presence of 50% PEG 600, 0.1 M CHES pH 9.5, and 0.1 mM $CoCl_2$. H82A crystals were obtained from 30% v/v 2-propanol, 0.1 M Hepes pH 7.5, 0.2 M $MgCl_2$, 10 mM spermidine and 0.1 mM $ZnCl_2$. Diffraction experiments were performed at the beamline 4A of Pohang Accelerator Laboratory, Korea, and beamline PF-5A of Spring-8, Japan. The crystal structure of the zinc-bound PaAP was determined by molecular replacement. The monomeric structure of human aspartyl aminopeptidase (PDB id: 4DYO), which shares 41% sequence identity with PaAP, was used as a search model. Other three structures were determined by molecular replacement using the zinc-bound PaAP as a template. Data collection and refinement statistics are shown in Table 1. The detailed procedures for crystallization and structure determination were described in Supplementary materials.

2.3. Hydrolysis activity of PaAP

Aminopeptidase activity assay for PaAP was performed as described previously [17] with modifications. The purified PaAP with the concentration range from 0.5 to 5.0 μM was incubated in an assay mixture containing 0.1 M Hepes-NaOH pH 7.5, 0.1 mM of transition metal, and aspartyl-*p*-nitroanilide with the various concentrations up to 5 mM at 37 °C. The enzyme activity was monitored by measuring the absorbance of the released *p*-nitroaniline as a product at 405 nm. The detailed experimental conditions are described in Supplementary materials.

3. Results and discussion

3.1. Effects of transition metal ions on kinetic values and substrate specificities

In contrast to the human and mammalian M18 aspartyl aminopeptidases which have the angiotensin as a physiological target system [4,6], the suitable physiological substrate for PaAP is not well known. Therefore, we attempted quantitative assay of PaAP

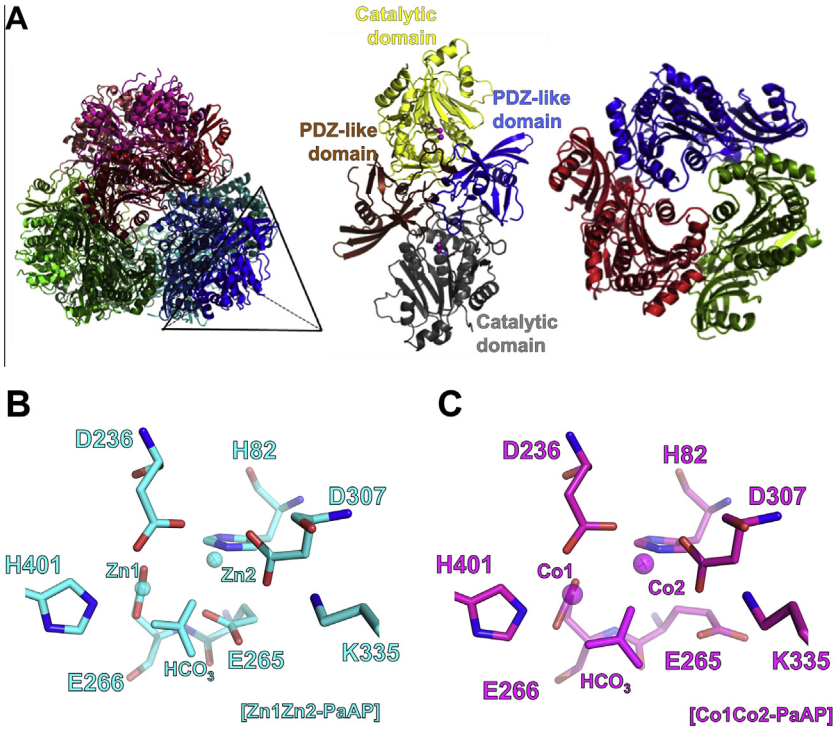

Fig. 2. Crystal structures of PaAP. (A) From left to right, ribbon representations of PaAP dodecamer, dimer, and trimer. Each subunit in dodecamer and trimer is colored differently. In a dodecameric structure, a tetrahedron represents an asymmetric unit which contains four PaAP monomers. In the PaAP dimer, the PDZ-like domain and catalytic domain in one monomer are colored brown and yellow, respectively, and those of the other monomer are colored blue and grey, respectively. Two metal ions in catalytic site are represented by magenta balls. The three fold operation of four trimers reveals the dodecameric structure. The bimetal catalytic sites of [Zn1Zn2-PaAP] (B) and [Co1Co2-PaAP] (C). Residues involved in metal coordination, metals and bicarbonate ion are represented by cyan and magenta stick models and labeled for [Zn1Zn2-PaAP] and [Co1Co2-PaAP] structures, respectively.

activity with aminoacyl-*p*-nitroanilides as substrates since these substrates were successfully introduced as a substrate of the assay for M18 aspartyl aminopeptidase of *Aspergillus oryzae* [17]. When the catalytic activities of purified recombinant PaAP with various transition metal ions such as Mn^{2+}, Co^{2+}, Ni^{2+}, Cu^{2+}, and Zn^{2+} were measured, Co^{2+} and Mn^{2+} conferred higher activities than did Zn^{2+} (Table 2). The catalytic reaction constant, k_{cat} (s^{-1}) of PaAP is 0.43 ± 0.05 in the presence of Zn^{2+}, while the apo-enzyme showed almost zero activity. However, the k_{cat} value dramatically increased to 5.10 ± 0.33 with Co^{2+}. Mn^{2+} also conferred activation to a level similar to that of Co^{2+}, while Ni^{2+} and Cu^{2+} conferred lower activation than did Co^{2+} or Mn^{2+}.

To further examine the metal preferences of the clan MH peptidases, we investigated the glutamyl aminopeptidase of *Streptococcus pneumonia* (SpGP, also known as PepA) [18] which belongs to aminopeptidase family M42 in clan MH, and found that the activation specificity for the same series of metal ions to SpGP has considerable identity with that of PaAP. Like M18 PaAP, M42 SpGP was highly activated by Co^{2+} and Mn^{2+}, but not by Zn^{2+} (Table 2). If these increments in k_{cat} values were observed only under conditions of maximal substrate concentration ([S0] ≫ K_M), the apparent activity would only represent their *in vitro* biochemical functioning. However, the metal specificities represented by k_{cat} changes are also seen in the k_{cat}/K_M values (Table 2), demonstrating that clan MH peptidases would be highly activated with Co^{2+} or Mn^{2+} even in physiological conditions [8]. To investigate the substrate specificity of PaAP, we examined the enzymatic activity of PaAP using various substrates in the absence of metal ions, in the presence of Co^{2+}, or Zn^{2+}. Apoenzyme showed almost negligible activity, and thus substrate selectivity could not be evaluated. In the presence of Co^{2+}, PaAP displayed a significant preference for the negatively charged amino acids, Asp and Glu, as expected (Fig. 1). However, in the presence of Zn^{2+}, catalytic activity of PaAP on the negatively charged residues was dramatically reduced, and thus its substrate preference for the negative charged residues was not significant (Fig. 1). Although PaAP is classified as an aspartyl aminopeptidase of the M18 peptidase family [2,16], it also showed high activity against glutamate, suggesting that PaAP is an aminopeptidase having preference for the negatively charged residues as substrates. Interestingly, another member of the M18 peptidases, yeast aminopeptidase I, has broad substrate specificity [3], and *Pyrococcus furiosus* M18 even exhibits Lys-specific activity [19]. These results indicate that M18 peptidases, having diverged from their common ancestor, have diverse substrate specificities.

3.2. Structural analysis of PaAP

To understand the basis of metal-specific activation of PaAP, crystal structures of PaAP were determined in the presence of Zn^{2+} at 2.3 Å resolution and Co^{2+} at 2.7 Å resolution (Table 1). The presence of metal ions in the crystals was confirmed by X-ray fluorescence scan at beamline 4A, Pohang Accelerator Laboratory, Korea, with peaks of 9.68 (keV) for Zn^{2+} and 7.71 (keV) for Co^{2+}. Four monomers of PaAP in an asymmetric unit form a dodecameric tetrahedron structure by crystallographic three-fold symmetry operation in the *H3* space group (Fig. 2A). Therefore, it belongs to a member of dodecameric tetrahedral (TET) protease family. Each monomer consists of a PDZ-like domain which is involved in subunit interaction, and a catalytic domain which contains the catalytic active site with two metal binding sites (M1 and M2 sites) for cocatalytic and structural metal ions, respectively (Fig. 2A). Therefore, Zn^{2+}- and Co^{2+}-bound structures are designated as [Zn1Zn2-PaAP] and [Co1Co2-PaAP], respectively, where cocatalytic and structural metals are sequentially numbered (Fig. 2B and C). The structural architecture of the oligomer and the subunit structure are similar to those of mammalian aspartyl aminopeptidase, bovine AP (bAP) and human AP (hAP) [6,16] which also belongs to the M18 family. The root mean square deviation (rmsd) between [Zn1Zn2-PaAP] and [Zn1Mg2-bAP] (PDB ID: 3VAT) is 1.08 Å for 408 Cα atoms (Fig. S1). [Zn1Zn2-PaAP] contains two zinc ions separated by 3.4 Å in the bimetal catalytic site. In addition, the positive electron density near the metal was modeled as bicarbonate ion, since it fits well into the electron density. The concentration of bicarbonate ion in Tris buffer at room temperature is known to be close to 4 mM [20], which supports the possible presence of bicarbonate ion in the active site of PaAP. Bicarbonate ion is also found in more than 100 crystal structures deposited in the protein data bank. Interestingly, bicarbonate ion was also found in the active site of leucine aminopeptidase [10]. However, the bicarbonate ion seems to not work as base to nucleophilic water in PaAP, as proposed for leucine aminopeptidase, since the addition of bicarbonate ion did not increase the catalytic activity of PaAP (Fig. S2). The cocatalytic zinc ion (Zn1)

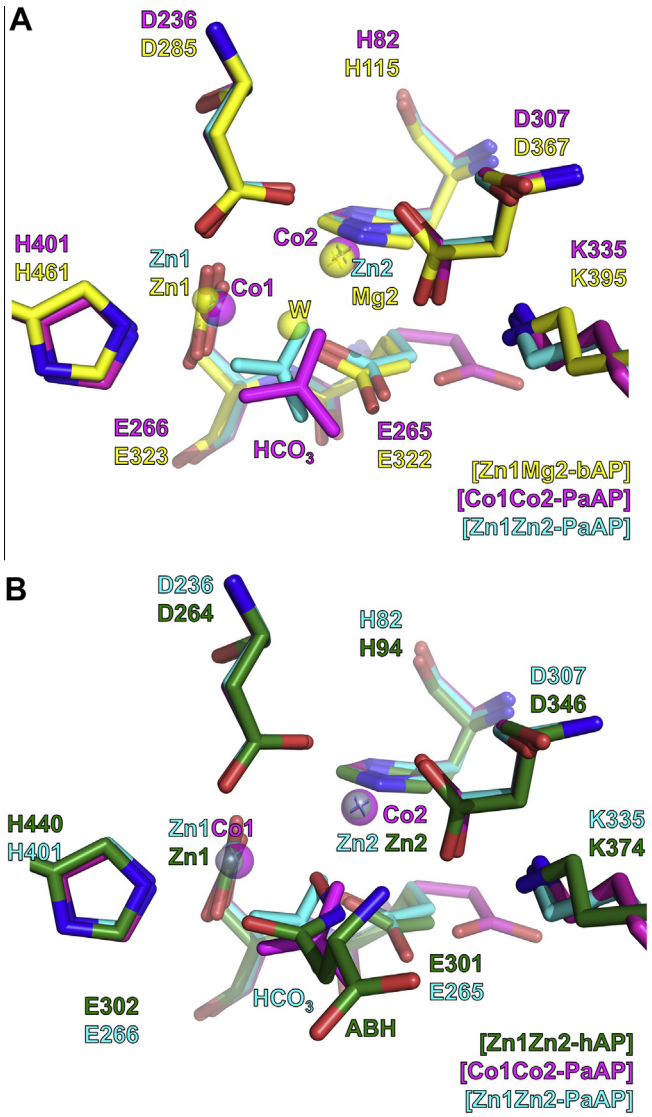

Fig. 3. Structural alignment of *P. aeruginosa* aspartyl aminopeptidases (PaAP) with bovine and human aspartyl aminopeptidases. (A) Structural overlap of [Zn1Zn2-PaAP] and [Co1Co2-PaAP] with [Zn1Mg2-bAP] (PDB ID: 3VAT), which are drawn as stick models with cyan, magenta and yellow colors, respectively. (B) Structural superposition of [Zn1Zn2-hAP] (PDB ID: 4DYO) with [Zn1Zn2-PaAP] and [Co1Co2-PaAP], drawn as green, cyan, and magenta stick models, respectively. ABH molecule bound to the active site of [Zn1Zn2-hAP] is also drawn as a stick model and labeled.

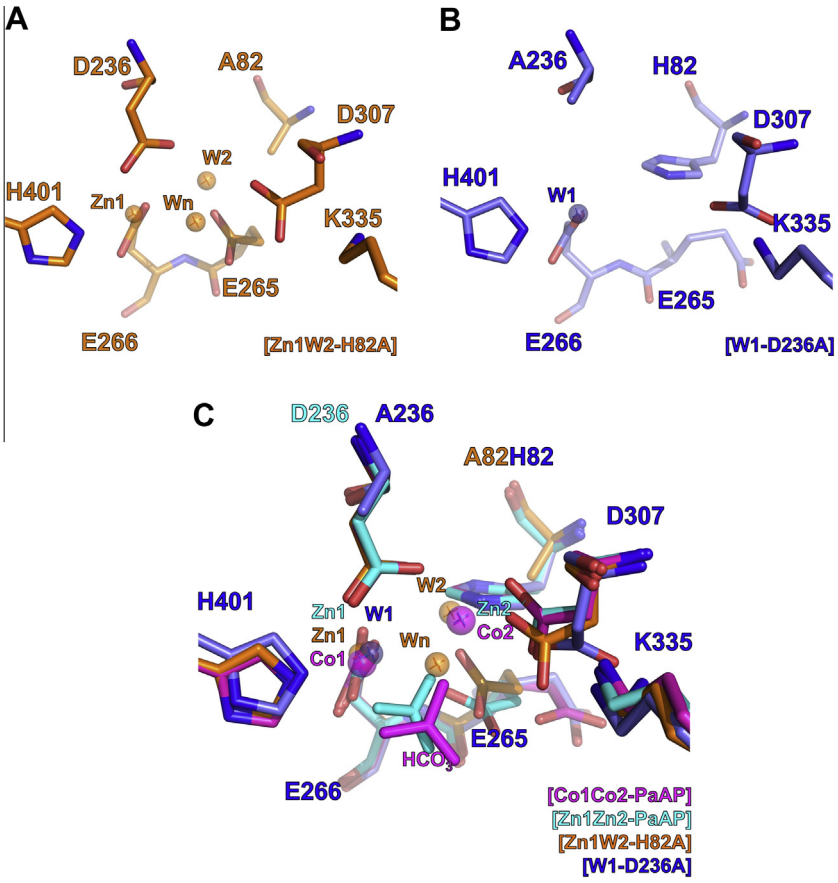

Fig. 4. The bimetal catalytic sites of [Zn1W2-H82A] (A) and [W1-D236A] (B). The color schemes and labels are orange and blue for [Zn1W2-H82A] and [W1-D236A], respectively. The water molecules in the position of nucleophilic water and M2 site are labeled as Wn and W2, respectively. (C) Structural alignment between [Zn1Zn2-PaAP], [Co1Co2-PaAP], [Zn1W2-H82A] and [W1-D236A] with the same color schemes in Figs. 3 and 4(A)(B).

Table 3
Michaelis-Menten parameters and reaction constants for PaAP mutants D236A, H401A and H82A.

Enzyme	k_{cat} (s^{-1})			k_{cat}/K_M ($s^{-1}M^{-1}$)			K_M (mM)		
	No metal	Co^{2+}	Zn^{2+}	No metal	Co^{2+}	Zn^{2+}	No metal	Co^{2+}	Zn^{2+}
D236A	0.003 ± 0.0002	0.03 ± 0.001	0.005 ± 0.0001	5	113	47	0.51 ± 0.04	0.26 ± 0.04	0.10 ± 0.01
H401A	0.03 ± 0.0003	0.25 ± 0.02	0.02 ± 0.002	45	589	67	0.56 ± 0.15	0.42 ± 0.05	0.37 ± 0.07
H82A	0.02 ± 0.002	0.88 ± 0.03	0.02 ± 0.001	43	1076	61	0.41 ± 0.08	0.82 ± 0.07	0.42 ± 0.09

is coordinated by His-401, Asp-236, Glu-266, and bicarbonate ion, while the structural zinc ion (Zn2) is coordinated by His-82, Asp-236, Asp-307, and bicarbonate ion (Fig. 2B, Table S1). Therefore, three amino acids and HCO_3^{2-} create the tetragonal coordination geometry for the metal ions. The [Co1Co2-PaAP] structure is almost identical to the [Zn1Zn2-PaAP] structure with rmsd of 0.44 Å for 409 Cα atoms (Fig. S1). In the [Co1Co2-PaAP] structure, two cobalt ions separated by 3.3 Å are also coordinated by the bicarbonate ion and the same residues as in [Zn1Zn2-PaAP] with the tetragonal geometry (Fig. 2C, Table S1).

3.3. Structural comparison with bovine and human APs

In PaAP, Glu-265 seems to have a role as a general base to facilitate the nucleophilic attack on the scissile bond by activating the nucleophilic water, since it structurally overlaps with bases in other bimetallic aminopeptidases (Fig. 3). In the [Zn1Zn2-PaAP] structure, one of bicarbonate oxygen atoms is placed on the position of a nucleophilic water molecule in the [Zn1Mg2-bAP] structure (Fig. 3A) and also forms bonds with two metal ions as well as Glu-265. Therefore, this bicarbonate oxygen is assumed to be located on the nucleophilic water. Interestingly, in the crystal structure of hAP in complex with aspartate-β-hydroxamate (ABH), a substrate analog, ABH forms a salt bridge to Lys-374 [16], corresponding to Lys-335 in PaAP (Fig. 3B). In the overlap structure of [Co1Co2-PaAP] with [Zn1Zn2-hAP], Lys-374 of hAP points to the ABH, suggesting that Lys-335 of PaAP is possibly involved in substrate recognition in PaAP. Previously, PaAP was predicted to show no activity on negatively charged substrates, due to the absence of Lys or Arg residues in its S1 binding pocket, based on sequence alignment with hAP [16]. However, our results provide the possibility that positively charged residues in PaAP form a S1 binding pocket, which explains why PaAP shows substrate specificity for negatively charged substrates.

3.4. Structural difference between the cobalt- and zinc bound PaAPs

Previously, it is hypothesized that the nucleophilicity or polarizability of the active site water, or pK_a of bases involved in water

deprotonation, might be affected by the coordinated metal, which could result in a metal-dependent change in activity [8]. In the case of bAP, Mn^{2+}-dependent activation was explained by electronic structure of metal ions as revealed by a change in the X-ray absorption edge spectra technique [6]. In other report, the polarization of nucleophilic water is hypothesized to be affected by the species of cocatalytic metals [21]. It has also been proposed for hAP that the coordination geometry of metals influences enzymatic activity [16]. To elucidate the structural bases of the metal-dependent activity change, [Zn1Zn2-PaAP] and [Co1Co2-PaAP] were compared (Fig. 3). No remarkable structural differences that could explain the metal-dependent activity change of PaAP were observed. However, it is revealed that bicarbonate ion as well as Glu-265 was moved away from Asp-236 in [Co1Co2-PaAP] although metal binding site is almost identical (Fig. 3). As a result, it is expected that the nucleophilic water moves closer to the substrate in the cobalt-bound structure. Therefore, it is tempting to hypothesize that the metal-dependent activity change might be correlated with the distance between the nucleophilic water and the substrate. More accurate biophysical examination will be required to elucidate the metal-activated property of water and its relevance to the catalytic activity.

3.5. Structural and functional analyses of PaAP mutants

To further understand the role of metal ions, PaAP mutants were designed to abolish the coordination of one or both ions. Asp-236 which is in coordination with both metal ions and His-82 coordinates which coordinates one metal ion were mutated. Crystal structures of mutants clearly demonstrated that D236A does not harbor metal ions and H82A has one metal ion in M1 site (Fig. 4), although overall conformations are well conserved: [Zn1Zn2-PaAP] has rmsd of 0.36 Å for 393 Cα atoms with D236A, and rmsd of 0.38 Å for 406 Cα atoms with H82A. Interestingly, D236A has a well-defined water in M1 site (Fig. 4A) and H82A contains a water in M2 site (Fig. 4B). Accordingly, we designated them as [W1-D236] and [Zn1W2-H82A], respectively. Functional investigation of mutants showed that D236A retained almost no activity regardless of metal species, while H82A showed considerable activity in the presence of cobalt ion (Table 3). Also the mutation of Glu-265, a putative general base, completely abolished the catalytic activity of PaAP (data not shown). These results confirmed that metal ions and Glu-265 are essential for the catalytic function of PaAP. In the crystal structure of [Zn1W2-H82A], a water molecule (Wn), found in the position of the nucleophilic water, is hydrogen-bonded with the general base, Glu-265 (Fig. 4B), suggesting that the catalytic site is well maintained although the metal ion in M2 site is missing. In contrast, H401A had lower activity than H82A. Although the crystal structure of H401A was not determined due to the difficulty of crystallization, H401A is expected to harbor a metal ion only in M2 site, considering its contribution to the metal coordination in M1 site. Taking these together, we propose that the metal ion in M1 site is crucial for the proteolytic function of PaAP. In addition, it is also suggested that the metal in M1 site is a key determinant of the metal preference of PaAP, since the turnover number was more affected by H82A than by H401A substitution (Table 3). Previously, His-94 of hAP, corresponding to His-82 of PaAP, was suggested to be essential for the catalytic activity, since H94F mutation abolished the activity [5]. But, our results revealed H82A retains some catalytic activity and its M1 site overlaps with that of [Zn1Zn1-PaAP], thereby suggesting that His-82 may perform an auxiliary role in catalysis (Fig. 4C). It is likely that the loss of activity in H94F of hAP was caused by conformation changes in the catalytic site due to the increased steric hindrance by Phe substitution.

3.6. Physiological relevance of Co^{2+} activation

For bacteria cultured in LB media, the intracellular concentrations of zinc and cobalt are estimated to be 10^{-1} mM and 10^{-4} mM, respectively [22], but their concentrations can vary when cells are exposed to different conditions [22–24]. Since Zn^{2+} is physiologically abundant, it is expected that PaAP is activated by Zn^{2+}. However, Zn^{2+} can be replaced by Co^{2+} when the local concentration of Co^{2+} is increased. Therefore, depending on the binding affinity of metals to PaAP and the relative concentrations of metals in given conditions, the cocatalytic metals normally bound to the active site of PaAP might be displaced by other metals. To address this argument at least partially, we examined the Co^{2+}-dependent activity of PaAP in the presence of a saturating concentration of Zn^{2+} (Fig. S3). A low concentration of Co^{2+} (0.01–0.1 mM) can make PaAP fully active even in the presence of an excess of Zn^{2+} (0.1 mM), demonstrating that Co^{2+} may supersede Zn^{2+} and act as a regulator of M18 in specific biological environments.

In summary, we observed that the catalytic activities of PaAP and SpGP aminopeptidases were highly enhanced by Co^{2+}. Structural comparison between Zn^{2+}- and Co^{2+}-bound PaAP structures revealed subtle structural changes such as the movement of the nucleophilic water and general base, which proposes the possibility that the differential positioning of the nucleophilic water may account for the metal-dependent activity changes. In addition, we propose that M1 site primarily determines the metal preference among the two metal binding sites. Based on our current observations together with the metal preferences of other known aminopeptidases, we propose that Co^{2+} can be described as a cocatalytic metal ion for clan MH peptidases.

4. Accession numbers

The atomic coordinates and structure factors were deposited in the Protein Data Bank with the accession codes 4NJR, 4NJQ, 4OID, and 4OIW for coordinates of zinc-bound, cobalt-bound, D236A mutant, and H82A mutant PaAPs, respectively.

Acknowledgments

This work was supported by R&D Convergence Center Support Program, Ministry of Agriculture, Food and Rural Affairs, and National Research Foundation of Korea Grant (2011-0028878) to K.K., and the National Research Foundation of Korea grant (2011-0013663) to H.J.Y.

Appendix A. Supplementary data

Supplementary data associated with this article can be found, in the online version, at http://dx.doi.org/10.1016/j.bbrc.2014.03.109.

References

[1] N.M. Hooper, U. Lendeckel, Aminopeptidases in Biology and Disease (Proteases in Biology and Disease), Springer, New York, 2004.
[2] N.D. Rawlings, A.J. Barrett, A. Bateman, MEROPS: the database of proteolytic enzymes, their substrates and inhibitors, Nucleic Acids Res. 40 (2012) D343–D350.
[3] Y.H. Chang, J.A. Smith, Molecular cloning and sequencing of genomic DNA encoding aminopeptidase I from *Saccharomyces cerevisiae*, J. Biol. Chem. 264 (1989) 6979–6983.
[4] S. Wilk, E. Wilk, R.P. Magnusson, Purification, characterization, and cloning of a cytosolic aspartyl aminopeptidase, J. Biol. Chem. 273 (1998) 15961–15970.
[5] S. Wilk, E. Wilk, R.P. Magnusson, Identification of histidine residues important in the catalysis and structure of aspartyl aminopeptidase, Arch. Biochem. Biophys. 407 (2002) 176–183.
[6] Y. Chen, E.R. Farquhar, M.R. Chance, K. Palczewski, P.D. Kiser, Insights into substrate specificity and metal activation of mammalian tetrahedral aspartyl aminopeptidase, J. Biol. Chem. 287 (2012) 13356–13370.

[7] F. Teuscher, J. Lowther, T.S. Skinner-Adams, T. Spielmann, M.W. Dixon, C.M. Stack, S. Donnelly, A. Mucha, P. Kafarski, S. Vassiliou, D.L. Gardiner, J.P. Dalton, K.R. Trenholme, The M18 aspartyl aminopeptidase of the human malaria parasite *Plasmodium falciparum*, J. Biol. Chem. 282 (2007) 30817–30826.
[8] W.T. Lowther, B.W. Matthews, Metalloaminopeptidases: common functional themes in disparate structural surroundings, Chem. Rev. 102 (2002) 4581–4607.
[9] V.K. Antonov, L.M. Ginodman, L.D. Rumsh, Y.V. Kapitannikov, T.N. Barshevskaya, L.P. Yavashev, A.G. Gurova, L.I. Volkova, Studies on the mechanisms of action of proteolytic enzymes using heavy oxygen exchange, Eur. J. Biochem. 117 (1981) 195–200.
[10] N. Gomis-Rüth, L. Sun, E.R. Kantrowitz, W.N. Lipscomb, A bicarbonate ion as a general base in the mechanism of peptide hydrolysis by dizinc leucine aminopeptidase, Proc. Natl. Acad. Sci. USA 96 (1999) 11151–11155.
[11] M.P. Allen, A.H. Yamada, F.H. Carpenter, Kinetic parameters of metal-substituted leucine aminopeptidase from bovine lens, Biochemistry 22 (1983) 3778–3783.
[12] F.H. Carpenter, J.M. Vahl, Leucine aminopeptidase (Bovine lens). Mechanism of activation by Mg^{2+} and Mn^{2+} of the zinc metalloenzyme, amino acid composition, and sulfhydryl content, J. Biol. Chem. 248 (1973) 294–304.
[13] S. Himmelhoch, Leucine aminopeptidase: a zinc metloenzyme, Arch. Biochem. Biophys. 134 (1969) 597–602.
[14] K.W. Walker, R.A. Bradshaw, Yeast methionine aminopeptidase I. Alteration of substrate specificity by site-directed mutagenesis, J. Biol. Chem. 274 (1999) 13403–13409.
[15] M. D'Souza, V.R.C. Holz, The methionyl aminopeptidase from *Escherichia coli* can function as an iron(II) enzyme, Biochemistry 38 (1999) 11079–11085.
[16] A. Chaikuad, E.S. Pilka, A. De Riso, F. von Delft, K.L. Kavanagh, C. Venien-Bryan, U. Oppermann, W.W. Yue, Structure of human aspartyl aminopeptidase complexed with substrate analogue: insight into catalytic mechanism, substrate specificity and M18 peptidase family, BMC Struct. Biol. 12 (2012) 12–14.
[17] J. Watanabe, H. Tanaka, T. Akagawa, Y. Mogi, T. Yamazaki, Characterization of *Aspergillus oryzae* aspartyl aminopeptidase expressed in *Escherichia coli*, Biosci. Biotechnol. Biochem. 71 (2007) 2557–2560.
[18] D. Kim, B.H. San, S.H. Moh, H. Park, D.Y. Kim, S. Lee, K.K. Kim, Structural basis for the substrate specificity of PepA from *Streptococcus pneumoniae*, a dodecameric tetrahedral protease, Biochem. Biophys. Res. Commun. 391 (2010) 431–436.
[19] S.V. Story, C. Shah, F.E. Jenney Jr., M.W. Adams, Characterization of a novel zinc-containing, lysine-specific aminopeptidase from the hyperthermophilic archaeon *Pyrococcus furiosus*, J. Bacteriol. 187 (2005) 2077–2083.
[20] G.M. Platt, I.N. Bastos, M.C. Andrade, G.D.A. Soares, In silico experiments of carbon dioxide atmosphere and buffer type effects on the biomimetic coating with simulated body fluids, Adv. Mater. Phys. Chem. 2 (2012) 239–248.
[21] F.X. Gomis-Rüth, F. Grams, I. Yiallouros, H. Nar, U. Küsthardt, R. Zwilling, W. Bode, W. Stöcker, Crystal structures, spectroscopic features, and catalytic properties of cobalt(II), copper(II), nickel(II), and mercury(II) derivatives of the zinc endopeptidase astacin, J. Biol. Chem. 24 (1994) 17111–17117.
[22] C.E. Outten, T.V. O'Halloran, Femtomolar sensitivity of metalloregulatory proteins controlling zinc, Science 292 (2001) 2488–2492.
[23] C. Blériot, G. Effantin, F. Lagarde, M.A. Mandrand-Berthelot, A. Rodrigue, RcnB is a periplasmic protein essential for maintaining intracellular Ni and Co concentrations in *Escherichia coli*, J. Bacteriol. 193 (2011) 3785–3793.
[24] M.L. Ellison, J.M. Farrow III, W. Parrish, A.S. Danell, E.C. Pesci, The transcriptional regulator Np20 is the zinc uptake regulator in *Pseudomonas aeruginosa*, PloS One 8 (2013) e75389.